

Fatigue Crack Propagation in Ceramic Wheel Used For Gas Turbine

HAIDER HADI JASIM

Department of Chemical Engineering
University of Basrah
College of Engineering
raidhani73@yahoo.com

Abstract- This paper studies and compared the fatigue crack propagation rate da/dN for three kinds of ceramic wheel (model A, model B, and model C) made of Si_3N_4 ceramic with different additives used for gas turbine application. The stress intensity factor range was calculated using finite element method and then compared with analytical approximate approaches. Experimental fatigue test was carried out on the three specimens taken from the models. As a result, the types of additives effect on fatigue crack propagation rate. The model A has the highest da/dN values and model C exhibits the lower values of da/dN .

Keywords: Crack propagation rate, stress intensity factor, FEM, J-Integral, Si_3N_4 ceramic material, porosity.

Nomenclature

a : Crack length (mm).

E : Modulus of elasticity (GPa.).

f_i : Body force (N).

F_I : Factor depending on (a/r_1) .

f_x, f_y : Body force in X and Y direction in (N).

J: J-Integral values (kN/m).

K: Stress intensity factor ($MPa \cdot \sqrt{m}$).

ν : Poisson ratio.

K_{max}, K_{min} : Maximum and minimum stress intensity factor ($MPa \cdot \sqrt{m}$).

r_1, r_2 : Inside and outside radius (mm).

h: Thickness of disc (mm).

n_j : Normal vector .

t: Transpose of matrix.

T : Traction vector.

u_i : Displacement vector (mm).

u_x, u_y : Displacement in the X and Y direction (mm).

W: Strain energy density.

(X_i, Y_i) : Coordinate of node (i) (mm).

(X_o, Y_o) : Reference position of rotation.

$\frac{da}{dN}$: Fatigue crack propagation rate (mm/cycle).

σ_o : Tangential stress in center of disc

ρ : Density of material (kg/m^3). (MPa.).

ω_z : Rotating angular velocity (rad/s).

N: Number of fatigue cycles.

σ^t : Stress vector transpose (MPa.).

σ_{ij} : Stresses matrix (MPa.).

ϵ : Strain vector.

Γ : Boundary of domain.

Ω : Surface of domain.

I. Introduction

Because of their high strength, oxidation and corrosion resistance, high fracture energy and superior wear performance, advanced ceramic (silicon nitride Si_3N_4) are promising materials for use in high temperature application equipment's [1]. Rotating wheel in turbocharger, gas turbine engine and automobile engine are examples of these applications. Centrifugal force caused by frequent starting up and stopping the wheel, which might result in fatigue failure.

Since ceramic wheels are working for an extended service life, their fatigue resistance under service must be investigated.

Silicon nitride (Si_3N_4) ceramic have low fracture toughness and difficulty in machining. Various kinds of chemical composition of sintering additive are selected and add to improve the different properties that needs in engineering applications [2].

The fatigue test is quite possibly the most useful test one can conduct on ceramic material. It generates S-N curve, which characterizes a material's mechanical failures.

Fatigue can be divided into: low-cyclic fatigue, associated with large

stresses and high cyclic fatigue, characterized by loading, which causes stresses within elastic range of martial and many thousands of cycles of stress reverses before fracture occurs. Gilbert C. J. et al. [3] studied about cyclic fatigue properties of two monolithic high-toughness Si_3N_4 on ceramic material. Dusza J. et al. [4] determined the mechanical properties of three sets of ceramic with different microstructure cut out of Si_3N_4 gas turbine rotor discs made for automotive applications. Biljana M. et. al. [5] studied the failure problems on Si_3N_4 roller cam used in diesel engine.

The finite element method and J-Integral approaches has considerably attracted the researchers for predicting the stress intensity factor range (ΔK) which is an important parameter for estimating the life of the cracked structure material under cycling loading. Kubo S. et al. [6] studied the method and its validity of estimation ΔJ by the path integral and finite element simulation of crack growth in which crack closure was taken into account. Stine V. [7] showed that fatigue crack growth is a typical reliability concern in most engineering components and simulated crack growth numerically using advanced 2D and 3D extended finite element method. Dianyin H. [8] provides a new way to estimate the crack growth lifetime criterion of the turbine components under high-low cyclic fatigue loading using experimental and FEM methods.

In this paper, the fatigue crack propagation for three kinds of ceramic turbine wheel made from silicon nitride with different additives (Model A, model B, model C) was studied by using finite element method and analytical method. Fatigue test was carried on specimens of the three models to determine the S-N curves.

II. Finite Element Analysis and J-Integral

Fig.1 shows the photograph of three Si₃N₄ wheels which uses for test. Fig.2 shows example of elements division using 4-nodes isoperimetric element, dimensions and boundary conditions. The model consists of 400 element and 441 nodes. Special mesh using 3-nodes element will be used on crack and the number of element on crack will increase compared to other portion to increase accuracy. In FEM analysis, the specified upper and lower limit rotating speed was loaded onto three kinds of ceramic wheel, and analysis was made.

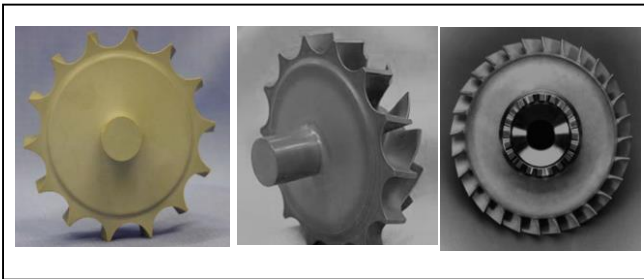


Fig. 1 Ceramic turbine wheels.

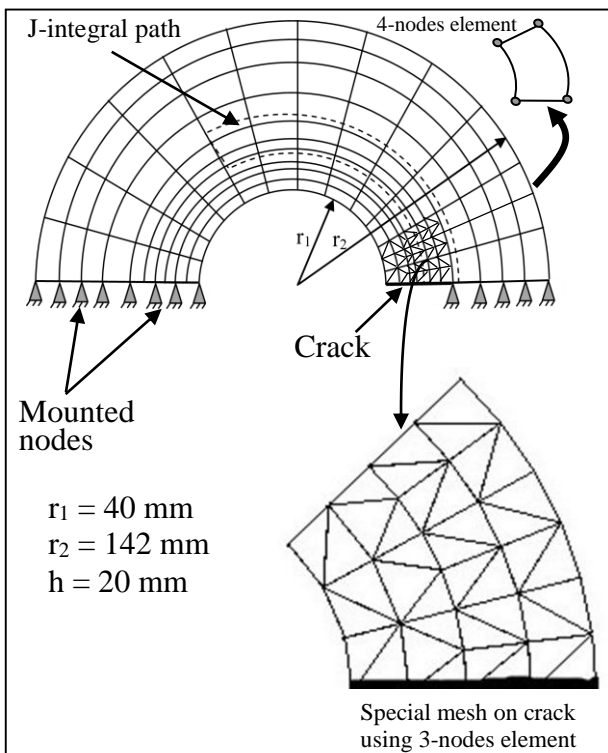


Fig. 2 Finite element division and J- Integral path.

The equation used in the calculation of J-Integral is [9]:

$$J = \int_{\Gamma} W dy - \int_{\Gamma} T^t \frac{\partial u}{\partial x} ds - \iint_{\Omega} f_i \frac{\partial u_i}{\partial x_i} dx dy \dots \dots \dots (1)$$

The strain energy is calculated from the following formula [10]:

$$W = \int_0^{\epsilon} \sigma^t d\epsilon = \frac{1}{2} \sigma^t \epsilon \dots \dots \dots (2)$$

In the case of a rotation about the Z-axis, the body force $f_i (\partial u_i / \partial x_i)$ of eq.1 can be expressed as follows [11] :

$$f_i \frac{\partial u_i}{\partial x} = f_x \frac{\partial u_x}{\partial x} + f_y \frac{\partial u_y}{\partial y} \dots \dots \dots (3)$$

Where,

$$f_x = -\rho (X_i - X_o)\omega_z^2 \dots \dots \dots (4)$$

$$f_y = -\rho (Y_i - Y_o)\omega_z^2 \dots \dots \dots (5)$$

Where (X_o, Y_o) reference position of rotation disc and equal to (0, 0).

The traction is defined as:

$$T = \sigma_{ij} n_j \dots \dots \dots (6)$$

In the analysis of fatigue loading of cracks the path independent J-Integral seems to be the most appropriate parameter. The reason is that uses nonlinearity on the crack tip. Unfortunately, the J-Integral cannot be applied to situations where unloading occurs (no internal stress/strain and no crack face tractions). This is due to the fact that J is based on the theory of deformation plasticity which represents plasticity by nonlinear elastic behavior.

Since the integral path independency for J-Integral is not guaranteed during unloading, the difference between maximum and minimum values of J-Integral during loading is defined the J-Integral range (ΔJ). The relation between J-Integral range and stress intensity factor range $\Delta K (K_{max} - K_{min})$ during cyclic loading is [12]:

$$\Delta J = \frac{(\Delta K)^2}{E} \dots \dots \dots (7)$$

The auto FEM software program version 2.2 developed by autoFEM LLP software company is used. The 4-nodes shell element was used for analysis of fatigue disc cyclic loadings. The finite element analysis is achieved in opening mode (mode I) fracture mechanics.

In order to run the autoFEM program, the following boundary conditions were applied:

- 1-The centrifugal forces are exerted due to disc angular velocity, i.e., the disc is mounted in Z-direction and rotated at the X-Y plane.
- 2- Null displacement in Y-direction in the mounting nodes and the nodes lie on the crack is free and have unknown displacements during cyclic loaded.

III. Stress Intensity Factor Calculation

For comparison a result obtained from auto FEM program, the stress intensity factor K_I for opening mode was calculated by the following theoretical formula [9, 13]:

$$K_I = \sigma_o \sqrt{\pi(r_1 + a)} F_I \dots \dots \dots (8)$$

Where,

$$\sigma_o = \frac{3 + \nu}{8} (r_2 \omega_z)^2 \rho$$

$$F_1 = 1.122 - 1.40\left(\frac{a}{r_1}\right) + 7.33\left(\frac{a}{r_1}\right)^2 - 13.08\left(\frac{a}{r_1}\right)^3 + 14.0\left(\frac{a}{r_1}\right)^4$$

IV. Material Properties

The material tested for this study was silicon nitride ceramic with different types of additives named (Model A, Model B and Model C). Tensile properties and chemical compositions for these kinds of materials are listed in table1 and table2 respectively [3].

Table I Mechanical properties of the material tested [3].

Property	Models		
	Model A	Model B	Model C
E(GPa.)	271	260	294
v	0.34	0.3	0.28
ρ (kg/m ³)	5150	3000	3210
Strength (Mpa.)	700	600	1000

Table II Chemical composition of the three-disc material used [3].

Materials	Models		
	Model A	Model B	Model C
mgo	1.2	2	4
CaO	0.1	0.1	-----
Al ₂ O ₃	0.5	0.7	-----
Fe ₂ O ₃	0.7	0.2	-----
Y ₂ O ₃	-----	-----	6
ZrO ₂	-----	-----	0.5

V. Fatigue Test

Identical samples machined in accordance with the standards set by the ISO Code 1143 [14, 15] as shown in Fig.3 were loaded into an Instron RR Moore high-speed rotating fatigue tester shown in Fig.4. The Instron machine has a loading capacity of 9 to 101 lb, and a maximum speed of 10,000 RPM.

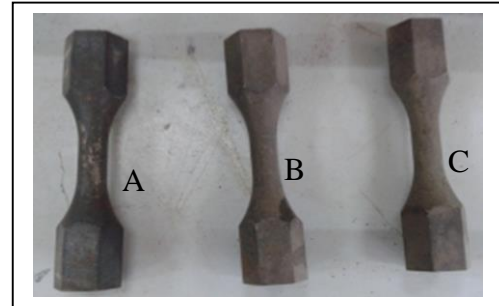
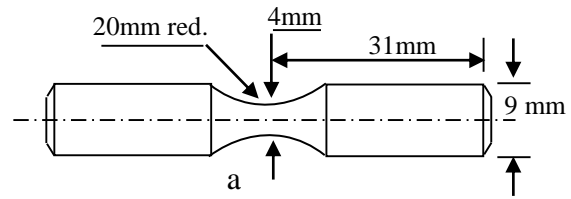


Fig. 3 a- Specimen dimensions
b- Specimen photograph for test.

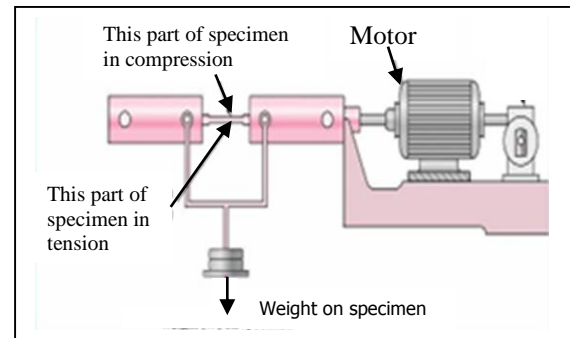


Fig. 4 Rotating-beam fatigue test machine [16]

Specimen rotating action is driven by a motor on the right results in tensile stress in the lower part and compressive stress in the upper part of the specimen gauge length. The gauge length of the specimen will be subjected to alternating tensile and compressive stresses as reversed cyclic loading. The specimen will be fatigue loaded until failure. The number of cycles to failure according to the cyclic stress applied will then be recorded.

Total 15 samples were tested until failure occurs. The fracture surfaces were observed using a computerize Carl Zeiss Jena imaging system, provided by camera smart technical have (22 Mega pixels). The test was achieved at Mech. Eng. Dep. Laboratory, Baghdad University.

VI. Results and Discussion

Fig.5 shows the number of fatigue cycle as a function of the applied stress amplitude. From the above Fig., it can be shown that there is a marked decrease in stress amplitude with increasing fatigue life. Damage increases proportional to the number of load cycles and this decreases material strength which leads to decrease stress amplitude.

Fig.6 shows fatigue crack length vs. number of cycles obtained from FEM using (autoFEM LLP software) and analytical methods (which is given by ref.8). As illustrated, all three models of wheels demonstrated the same

propagation behaviors until they caused fatigue fracture. The fatigue crack length was rather small for model A at the first cycle. There is a small difference in maximum values of fatigue crack length for model A and model B at final cycle, while model C give high values for fatigue crack length. The values of fatigue crack length obtained from autoFEM program for models A, B and C are (6.66, 5.1, and 4.23) mm while that obtained from analytical are (6.32, 4.64 and 4.05) mm respectively. This behavior attributed to the types and quantity of different additives added for each type of models. The additives makes cracks and defects move easily in model C compared to the models A and B. consequently, Model A have high and best resistance to crack extension as well as very high strength compared to models B and C.

The da/dN values were calculated with crack propagation curves in Fig.7 by means of the tangential method. Drawing tangential lines to each curve at different points and then calculating the slope of each line of Fig.6 at these different points along the curve, then, the value of slope of line are obtained and represented the crack propagation rate da/dN . The relationships between da/dN and ΔK of three models of rotating wheels are illustrated in Fig.7. These results obtained from analytical and FEM methods with specimen have the same dimensions for three models. In analytical method, the values of ΔK is calculated from the difference ($K_{max} - K_{min}$). K_{max} represent a highest algebraic value of the stress-intensity factor in a cycle and it is obtained from eq.8, while $K_{min} = 0$ (no loading applied). It was observed that all models show similar slop and the value of the da/dN increases for all models and have high values at the final stage of testing.

In viewing microscopic photographs of fracture surface of the specimens in Fig.8, it was observed that a large difference in fracture surface between models containing different additives.

The microstructure fracture surface of model A shows extensive porosity and cavities in the majority of the specimen surface and these considers the major cause of crack initiation and subsequently growth. Pores reduce the time for crack initiation by creating a high stress concentration in the material adjacent to the pores. Model B shows more edge places for cracks initiation compared to model A and also show mechanical damage.

In model B fracture surface shows that fatigue cracks initiate from many places and there are obvious wide fatigue striations in the crack initiated region. The mechanical damage is due to rotating bending load that develops the highest stress on the surface. Model C has smooth surface and less porosity compared to others.

In all three samples, it was observed that the edges in general had rougher surfaces than other parts of the cross-section. This suggests that fracture began before cracks could completely propagate through the material, which indicates the fracture strength of the material which was reached before the crack was completed.

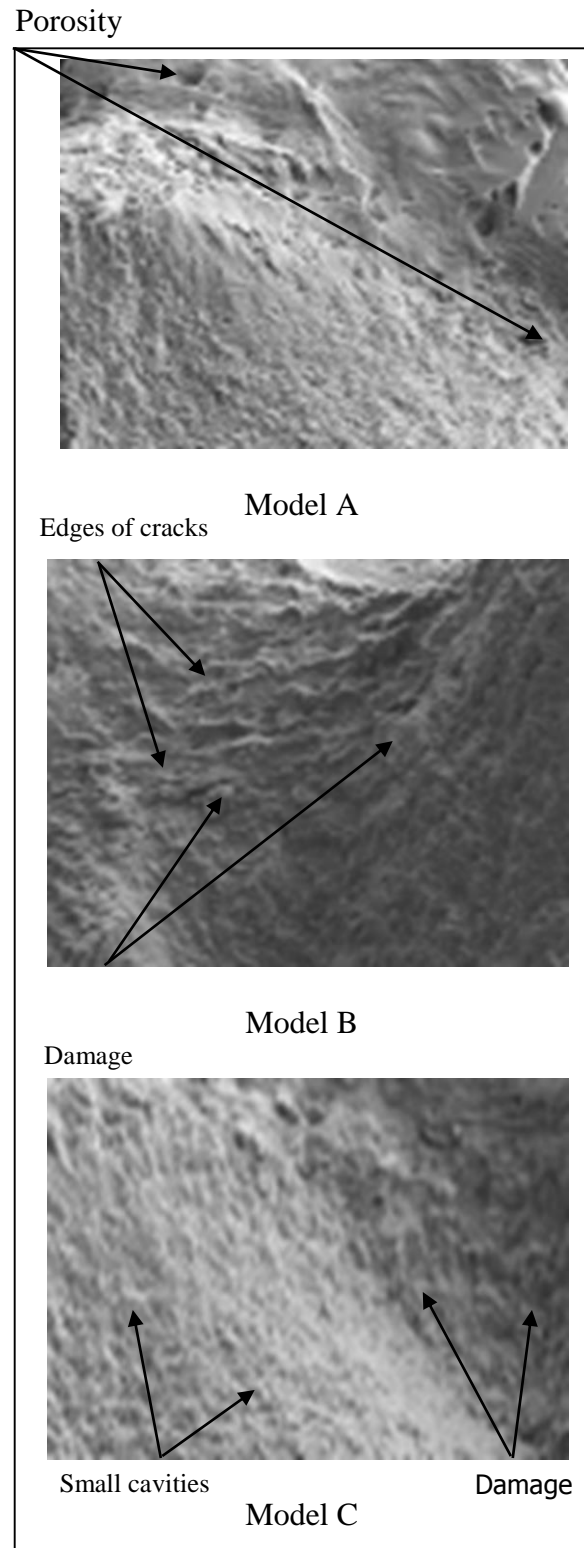


Fig. 8 Microscopic photographs of the fracture surfaces of three models.

VII. Conclusions

Based on a study of the fatigue crack propagation rate, J-Integral range and stress intensity factor range, remarkable conclusions can be obtained:

- 1-It observed that the fatigue crack propagation rate may be significantly influenced by the properties and types of additives.
- 2- The model A has the highest da/dN values while; the model C exhibits the lower values of da/dN.
- 3- Fatigue cracks in silicon nitride ceramic disc do not appear to initiation naturally, but is invariably associated with some pre-existing defects.
- 4-The results indicate that increasing the stress amplitude will lead to an increase crack propagation rate and reduce the number of cycles that it will take to fatigue the materials.
- 5- Fracture surface of model A shows more porosity and cavities, while, model B shows more crack initiation edges and model C shows very small cavities and less crack initiation edges.

VIII. Acknowledgement

The author expresses all thanks to Mat. Eng. Dept., Basrah University and to staff engineer at Al-Zabier gas station of electrical generation for their helps. The author expresses thanks to Mech. Eng. Dept., Baghdad University.

IX. References

- [1] Wijian To "Application of silicon nitride (Si_3N_4) ceramic in ball bearing", MEDIA MESIN, Vol. 15, No. 1, pp.17 – 25, 2014.
- [2] Gurpreet K. "Experimental and numerical analysis of tensile testing" M. SC. Thesis, Dep. of Mech. Eng., Thapar institute of Eng. Technology, Deemed University, Patiala, 2009.
- [3] Gilbert C. J., Y.S. Han, and D.K. Kim, "Anomalous cyclic fatigue-crack propagation behavior of small cracks in monolithic grain bridging ceramic", J. of ceramic Int., Elsevier science, Vol.26, No.7, pp.721-725., 2000.
- [4] Dusza G., T. Lube, R. Danzer and K. Lwesskoff, "Mechanical properties of some Si_3N_4 automotive gas turbine rotor ceramics", Key Engineering materials, Vol.89, No.91, 1994.
- [5] Biljan M., M. John, B. Edwin, M. Andree, "Silicon nitride applications in modern diesel engine", SAE Technical paper, No.1448, 2004.
- [6] Kubo S., T. Yafuso, M. Nohara, T. Ishmuro, and K. Ohaji, " Investigation on path integral expression of the J-Integral range using numerical simulation of fatigue crack growth", JSME , Series A, Vol.32, No.32, 1989.
- [7] Stine Vethe "Numerical simulation of fatigue crack growth", M. SC. Thesis, Norwegian University of Science and Technology, 2012.
- [8] Dianyin Hu, Rongqiao Wang, Huawei Liu, Jiaming Wei "Crack Growth Life Assessment on Turbine Component under Combined Fatigue Loading", 13th Int. Conference on Fracture, Beijing, China, 2013.
- [9] Shikida M., Sakane M., and Ohnami M., "Fatigue crack propagation for cast iron rotating disk", JSME International journal, series A, Vol.38, No.1, 1995.
- [10] Ivana V. Vasovi, Stevan M. Maksimovi, Dragi P. Stankovi, Slobodan N. Stupar, Mirko S. Makimovi and Gordana M. Baki "Fracture mechanics analysis of damage turbine rotor disc using finite element method ", Thermal science , Vol.18, pp. 107-112, 2014.
- [11] Ameen A. N. Al-Edani, "Efficient Fracture Mechanics Programming system for Linear and Non-Linear Problems Using Finite-Element and Boundary-Element Methods", Ph.D. Thesis, Cranfield Institute of Technology, England, 1990.
- [12] Wuthrich C., "The extension of J-Integral concepts to fatigue cracks", International Journal of fracture, Vol.20, No.2, 1982.
- [13] Tateki Yufaso, Masaye Itokaso, Shiru Kubo and Kiyotsugo Ohji, "Evaluation of the J-Integral range of fatigue crack emanating from notches by simple estimation formula" JSME Int. Journal, Vol.33, No.1, 1995.
- [14] Bernard G. L., O. M. Jadaan and L.A. Janosik, "Fatigue parameter estimation methodology for power and Paris crack growth law in monolithic ceramic material", NASA Technical paper, No.469, 1996.
- [15] International standard, ISO 1143-1975 (E): Metals Rotating Bar Bending Fatigue Testing.
- [16] Hashemi, S., Foundations of materials science and engineering, 4th edition, McGraw-Hill, 2006.

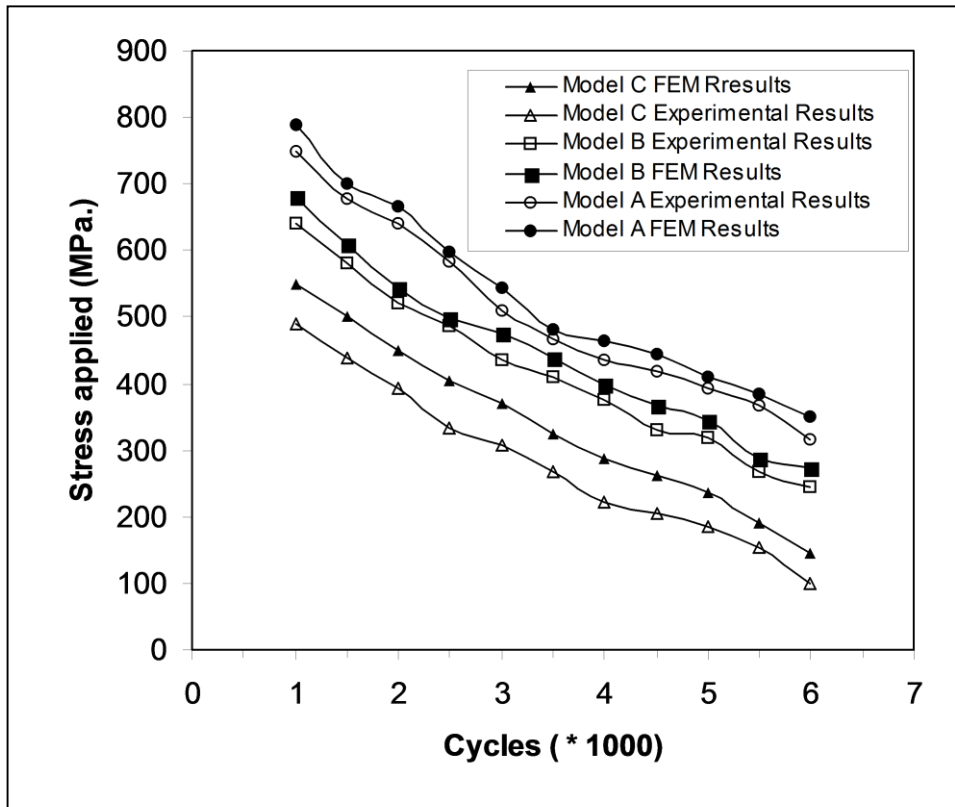


Fig. 5 Comparison of applied stress vs. cycles for three kinds of ceramic disc.

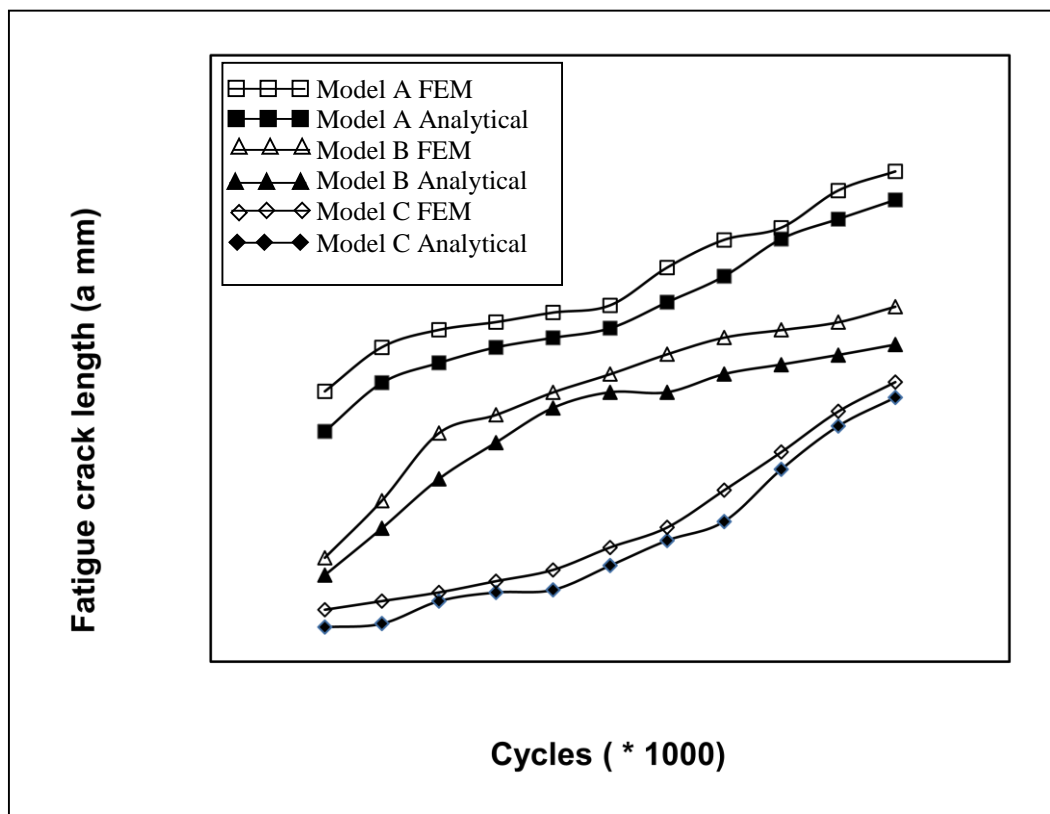


Fig. 6 Fatigue crack propagation for three kinds of ceramic materials.

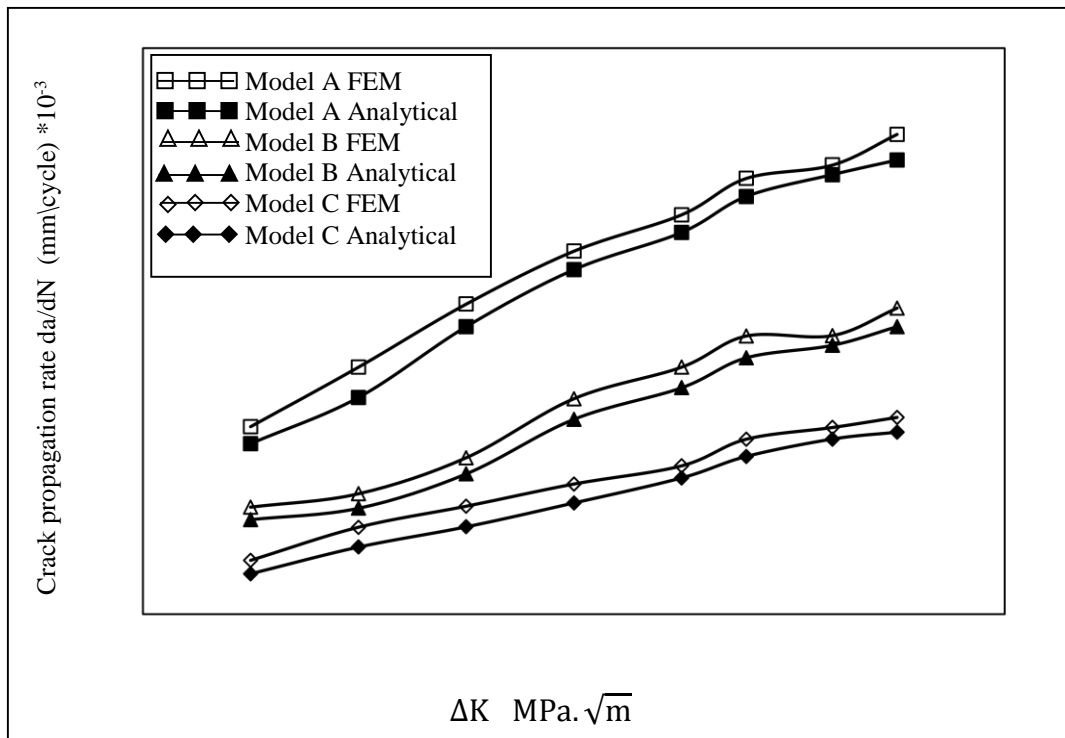


Fig. 7 Stress intensity factor range for three ceramic wheel materials.